

COMPARISON OF NITROGEN-DOPED PHOTOCATALYTIC SURFACES SYNTHESIZED BY PVD AND SOL-GEL METHODS

PRIMERJAVA FOTOKATALITIČNIH POVRŠIN, SINTETIZIRANIH S PVD IN SOL-GEL METODAMI

Erhan Ozkan*

Dikkan R&D Center, Izmir, Turkey

Prejem rokopisa – received: 2024-03-08; sprejem za objavo – accepted for publication: 2024-10-14

doi:10.17222/mit.2024.1132

The aim of this study was to produce photocatalytic $\text{TiO}_{2-x}\text{N}_x$ coatings that can be active in visible light using different methods. Physical vapour deposition (PVD) and sol-gel methods were preferred for these coatings. Thin films were synthesized by dip coating on a glass substrate using the sol-gel method. In addition, thin glass film coatings were obtained by applying an arc for one minute to the glass films using the PVD method. Since the coating phase is important in terms of photoactivity, a phase analysis was performed using XRD. The obtained surfaces will be used in antibacterial applications. Therefore, the thickness of the coatings was determined with the X-Ray refraction method, and their optical band gap was measured. Based on these values, it was observed that nitrogen has a reducing effect on the optical band gap in titanium oxide-based coatings. The aim of nitrogen doping was to enhance photoactivity by adding an additional band between the valence band and conduction band of a photocatalytic surface. After these experiments using rhodamine-B and methylene blue solutions, specimens' photocatalytic effects under fluorescent, sun and UV light were tested. It was determined that nitrogen's decreasing effect on the optical band gap results in increased photoactivity with both PVD and sol-gel techniques. In addition, it was found that the coatings made with PVD exhibited a more controlled structure in a shorter time, while the production of sol-gel coatings was a much cheaper method, with low investment costs.

Keywords: TiO_2 , sol-gel, PVD, photocatalysis, thin film

V članku avtor opisuje študijo izdelave fotokatalitičnih prevlek na osnovi $\text{TiO}_{2-x}\text{N}_x$, ki so lahko aktivne v območju vidne svetlobe. Prevele se lahko izdeluje z različnimi postopki. Avtor opisuje njihovo izdelavo s postopkom nanašanja v parni fazi (PVD; angl.: Physical Vapour Deposition) in tako imenovano Sol-Gel metodo izdelave tanke plasti s potapljanjem steklene podlage. Pri PVD metodi so tanko prevleko na stekleni podlagi dobili z delovanjem enominutnega obloka na stekleni film. S stališča fotoaktivnosti je fazna sestava prevlek pomembna, zato so izdelane prevleke, uporabne za antibakterijske aplikacije, analizirali z rentgensko difrakcijo (XRD). Debeline prevlek so bila določene z metodo loma in odboja rentgenskih žarkov. Izmerili so tudi širino optične pasovne reže. Na osnovi izmerjenih vrednosti je avtor opazoval učinek dušika na zmanjševanje širine optične pasovne reže na prevlekah, ki temeljijo na titanovem dioksidu (TiO_2). Razlog za dopiranje z dušikom je bil povečevanje fotoaktivnosti prevlek z dodajanjem dodatnega pasu med valenčnim in prevodnim pasom fotokatalitične površine. Po teh eksperimentih je avtor uporabil raztopini Rodamina-B in metilensko modre za testiranje vzorcev v fluorescenčni, vidni (sončni) in UV svetlobi. Z eksperimenti je potrdil zmanjševalni učinek dušika na širino reže optičnega pasu, kar je povzročilo povečanje fotoaktivnosti prevlek, izdelanih tako s PVD kot tudi s Sol-Gel tehnikami. Študija je tudi pokazala, da imajo PVD prevleke bolj kontrolirano mikrostrukturo in krajši čas aktivacije, medtem ko je izdelava prevlek s Sol-Gel postopkom cenejša in zahteva manjše investicijske stroške.

Ključne besede: titanov dioksid (TiO_2), postopka Sol-Gel in PVD, fotokataliza, tanki filmi

1 INTRODUCTION

The term photocatalysis describes reactions that are activated by light radiation. Since environmental pollution is an important problem in today's industrial world, research on photocatalysis is gaining in importance.¹⁻³ The decrease in natural water resources together with the pollution of the limited amount of domestic water due to industrial and environmental wastes has become one of the serious problems today's world.⁴ Chlorine used in water sterilization not only emits an irritating odour, but also causes the formation of harmful tri-halo-methane compounds, which can cause cancer as a result of the chemical reaction with the substances to be removed.⁵

Photocatalysis has gained prominence as an effective method for decomposing organic compounds in the system, addressing many of the above-mentioned problems. Photocatalysts are semiconductor materials that are activated by ultraviolet (UV) light and form a strong oxidizing environment.⁶ Bacteria and organic compounds stuck on the surface can be easily removed from the environment with the help of this oxidizing powder. In other words, photocatalysts are known as catalysts activated by the effect of light. By absorbing light, they reach a higher energy level and transfer the energy to the reactive material. In this way, a chemical reaction begins. An alloy of metal and semimetal can be used as a photocatalyst. Initially, Fe_2O_3 ,⁷ ZnO ,⁸ SrTiO_3 ,⁹ GaAs ,¹⁰ GaP ,¹¹ CdS ¹² and WO_3 ¹³ can be given as examples of semiconductor photocatalysts. The most widely used

*Corresponding author's e-mail:
erhan.ozkan@dikkan.com (Erhan Ozkan)

photocatalyst in applications is TiO₂ with an energy range of 3.2 eV.¹⁴ In order to change this range for different applications, Fe, Al, Cu, V, Pt, Cr, Ag and rare earth elements have been used.

TiO₂ based oxide films can be obtained with high investment costs and advanced technological equipment required for chemical vapour deposition,¹⁶ physical vapour deposition,¹⁷ and molecular beam epitaxy.¹⁸ However, they can also be synthesized with lower costs using the sol-gel technique for the synthesis of thin film coatings. This technique has advantages such as being able to control chemical reactions, obtaining a homogeneous structure, performing processes at low temperatures, low energy costs and not reacting with the substrate; however, there are also some disadvantages of producing TiO₂ thin films with the sol-gel method. These disadvantages include the fact that titanium alkoxide does not dissolve in most alcohols, the labour cost of the thin films produced with this method is high and takes a long time, the high shrinkage during synthesis, the presence of microporosities in the coating, and the processing with organic solvents that are harmful to health.^{19–22}

In this study, a titanium dioxide material with added nitrogen, intended for the production of a photocatalytic surface, used in antibacterial applications, was synthesized on glass surfaces using the sol-gel and PVD methods. The microstructures of the synthesized coatings were determined according to the phases identified with EDS and XRD, and their thermal and surface adhesion properties were investigated. Phase analyses of these coatings were performed using XRD, a thermal analysis was performed using DTA/TG, and surface structures were observed using SEM and AFM devices. According to the results, the coatings produced with the PVD technique showed good adhesion to the surface and a high deposition rate; they required low temperatures during deposition, and no additional heat treatment compared to the sol-gel technique. The aim of this study was to make a comprehensive comparison of the two methods – PVD, an expensive method, and sol-gel, a cheap and widely preferred method.

2 EXPERIMENTAL PART

2.1 PVD

A (30 × 40 × 3) mm quartz glass material was used as the base material. Glass samples were used because their optical properties could be measured. The purpose of using quartz glass was to prevent sodium migration into the coated film, otherwise encountered in normal glass, thus increasing photoactivity. For this purpose, preliminary preparations were made by passing the glass samples through acetone, isopropanol and pure water ultrasonic baths and then dried in an atmospheric environment with argon gas. Surface cleaning is based on removing particles from the sample surface by splashes caused by the high potential difference of argon gas emanating from the neutral molecule source.

Magnetic focus was used during the coating when the total pressure was $7.5 \cdot 10^{-3}$ torr, the total current was 50 A, and the duration was 1 min. The samples were covered at different nitrogen/oxygen ratios at room temperature, with a nitrogen gas flow of 60 sccm. **Table 1** shows different coating parameters.

Table 1: PVD coating parameters

Sample	Composition
1	TiN
2	50 % N ₂ – 50 % O ₂
3	25 % N ₂ – 75 % O ₂
4	15 % N ₂ – 85 % O ₂
5	10 % N ₂ – 90 % O ₂
6	5 % N ₂ – 95 % O ₂
7	Pure TiO ₂

2.2 SOL-GEL

In our experimental studies, titanium (IV) isopropoxide (Ti[OCH(CH₃)₂]₄, 99.999 % purity, Sigma Aldrich) as the starting material, ethanol (C₂H₅OH) as the solvent, hydrochloric acid (HCl) as the catalyst were used to obtain a TiO₂-based sol solution. Pure water (H₂O) was used for the hydrolysis of metal alkoxides. Hydrolysis and condensation reactions of titanium alkoxide are extremely exothermic forms a white precipitate in the presence of water or with moisture in the air. Therefore, acetyl acetone (C₅H₈O₂, at least 99 % purity, Merck) was used to control the reactions and avoid flash precipitates or the formation of an unstable colloidal solution during polycondensation. Urea (NH₂CONH₂, Merck) was preferred as the nitrogen additive. Two different solutions were prepared for the TiO₂ sol solution. To obtain the first solution, 1.5 mL of titanium (IV) isopropoxide was dissolved in 10 mL of ethanol by mixing them with a magnetic stirrer; then 0.35 mL of acetyl acetone was added and stirring was continued for 30 min. For the second solution, 0.92 mL of HCl, 0.15 mL of distilled water and 10 mL of ethanol were mixed. Then, these two solutions were combined, and mixing was continued for another 30 min. While preparing the doped TiO₂ solution, the additives were dissolved in 5 mL of ethanol at the determined rates and added to the main solution and the mixing process was continued. Additives were incorporated by setting the molar ratio of the additive starting material to the titanium starting material, and sample names were coded according to these ratios. In the experimental studies, the maximum solubility limit of urea used for the nitrogen additive in ethanol (RN: 2) and the additive ratios were determined by considering the literature.²³ Accordingly, the molar ratios of additives to titanium (IV) isopropoxide were determined for nitrogen, RN: 0.1, 1, and 2. The prepared solutions were kept at room temperature for one day and aged, and then the coating process was started.

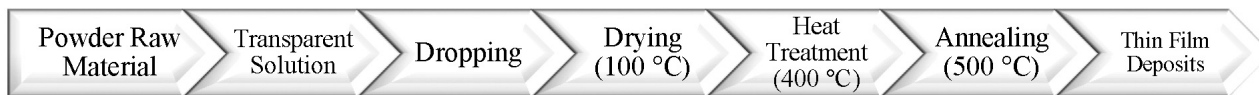


Figure 1: Workflow diagram of the process

SiO₂ interlayer coatings were applied to all samples in order to prevent the diffusion of alkali ions (Na⁺) in the soda-lime glass used as the substrate. Tetraethyl-orthosilicate (Si(OC₂H₅)₄, TEOS, 99.999 % purity, Sigma Aldrich) as the starting material for the SiO₂ interlayer film, ethanol (C₂H₅OH) as the solvent, hydrochloric acid (HCl) as the catalyst, and purified water (H₂O) for the hydrolysis of metal alkoxides were used in molar ratios of 1:4:0.3:4, respectively. In the preparation of SiO₂-based solutions, TEOS was first dissolved in ethanol by stirring it for about 30 min. Then, distilled water and hydrochloric acid were added, and mixing was continued for another 2 h. The solutions were aged at room temperature for 2 d. After the aging process, the prepared sol solutions were used to obtain thin films and powder photocatalysts. In order to prepare powder photocatalysts, sol solutions were dried at 100 °C for 24 h; water and alcohol were removed from their structures and samples in the xerogel form were obtained. For the thin film photocatalyst production, the prepared solutions were applied onto Corning® 2947 soda-lime glass surfaces using the dip coating method. Before the coating, the glass substrates were cleaned in an ultrasonic bath by holding them in acetone, ethanol, methanol and distilled water, respectively. During the coating, one side of the glasses was masked with a tape so that only one surface was covered. All the coatings were formed at an immersion speed of 100 mm/min in a Teknosem TDC-10 coating device. The coated glasses were dried in an oven at 100 °C. TiO₂ coatings were applied onto the substrates both with and without an SiO₂ interlayer. SiO₂ interlayer coated glasses were heat treated for 1 h at 500 °C in a Nabertherm furnace to ensure the crystallization of the interlayer coating before being used as the substrate.

Heat treatment at a rate of 10 °C/min was applied to obtain the anatase phase in doped and undoped TiO₂ thin films and powder samples. They were heat treated in the Nabertherm oven at 500 °C for 1 h, then rapidly cooled in a controlled manner at a rate of 5 °C/min. The process flow chart is given in **Figure 1**.

2.3 Characterization

Coating thicknesses were determined by X-ray refractometry. Thin-film geometry was used because the coating thickness was in the nanometer range. The θ angle was chosen as 0.5° and scans were made between 0.6° and 1.6°.

The crystal structure of thin-film coatings was investigated with a Phillips 3710 low-angle X-ray diffractometer under CuK α irradiation, at a 40 kV voltage and 40 mA current. Since the coating thickness was nano-

metres and the peaks were desired to be seen completely and clearly, the scanning speed was at 0.01 °/sec over 2θ angles from 20° to 120°.

Optical band gap measurement was made to get an idea about the activation energies of the coatings under visible light using the values found with the forbidden band energy measurement. An Aquila NKD device was used for the optical band gap measurement. With this device, the permeability and reflectivity of the material for each wavelength is graphically obtained by sending laser radiation at a constantly changing wavelength to the sample placed on the insole. These raw data obtained were likened to certain mathematical functions, from which the refractive index of sample n and extinction coefficient k were found. Using Equation (1), the absorption coefficient (α) was calculated in 1/meter.

$$\alpha = \frac{4k\pi}{\lambda} \quad (1)$$

After calculating the alpha value, the graphical method was used to calculate the forbidden band energy. For this, an energy value was first calculated using Equation (2).

$$E = \frac{hc}{\lambda} \quad (2)$$

The energy value calculated from the joule measurement was converted into eV units, and a graph of these values was drawn using Equations (3), (4) or (5) for each sample depending on whether the electron transition was indirect or direct. If the electrons were assumed to make an indirect transition, Equation (4) was used, and if they were assumed to be directly transferred, Equation (5) was used.

$$eV / \text{cm} = \alpha \frac{hc}{\lambda} \quad (3)$$

$$(eV / \text{cm})^2 = \left(\alpha \frac{hc}{\lambda} \right)^2 \quad (4)$$

$$\sqrt{(eV / \text{cm})} = \sqrt{\left(\alpha \frac{hc}{\lambda} \right)} \quad (5)$$

From the graph drawn in this way, a tangent is drawn from the end points where the curve becomes linear, and the point where these tangent cuts the horizontal axis gives the optical band gap of the material.

During the study of the coatings, photoactivity experiments were applied in three different ways. First, the visible light degradation of the methylene blue solution of the samples was investigated. In the second experiment, rhodamine-B solution was used and the effect of UV light was also investigated. In the next measurement,

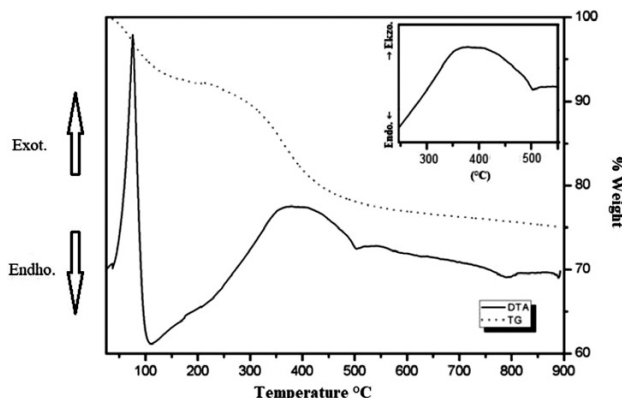


Figure 2: DTA/TG curve of the TiO₂ powders

the degradation of rhodamine-B was investigated in the samples under sunlight.

Methylene blue (C₁₆H₁₈ClN₃S) is a blue liquid, and the blue colour becomes lighter as its concentration decreases in the solution. The solution used had a concentration of 1.4×10^5 M. The samples were placed in a special test container with a gap of 18 cm under a fluorescent lamp (Philips TDL 18/54 Daylight) irradiated with a visible light of 18-Watt power. Seven coated glass samples and one uncoated glass sample were placed in the system. 10 mL of methylene blue solution was added to the samples. The initial absorbance of the solution was measured with a JASCO V-530 UV/VIS Spectrophotometer.

Rhodamine-B solution, which is more sensitive, was used to obtain more sensitive data in the studies under UV light. Rhodamine B is pink in colour and it lightens as its concentration in the solution decreases. The concentration of the solution used was 2 mg/lt.

3 RESULTS

Thermal properties of titanium oxide-based powders observed with a Perkin Elmer DTA/TG device under an

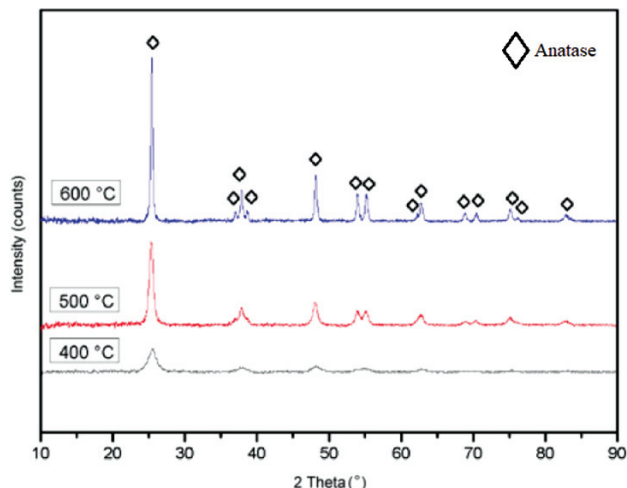


Figure 3: XRD results of unadulterated TiO₂ powders heat treated at different temperatures

argon atmosphere at a 100 ml/flow rate are shown in Figure 2.

Based on the TG/DTA results, annealed TiO₂ coatings' XRD patterns are given in Figure 3.

Microstructure properties of the coatings were determined with a Philips Excell 30 S FEG SEM device. Figure 4 shows SEM photographs of the coatings obtained with the sol-gel (left) and PVD (right) methods.

Coating thicknesses are given in Table 2.

Table 2: Coating thicknesses

Sample	Composition	PVD (nm)	Sol-gel (nm)
1	TiN	138	380
2	50 % N ₂ – 50 % O ₂	141	425
3	25 % N ₂ – 75 % O ₂	139	397
4	15 % N ₂ – 85 % O ₂	140	551
5	10 % N ₂ – 90 % O ₂	139	329
6	5 % N ₂ – 95 % O ₂	141	442
7	Pure TiO ₂	140	298

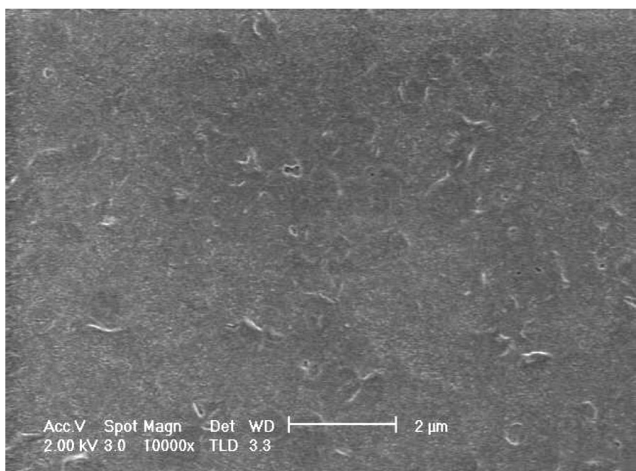
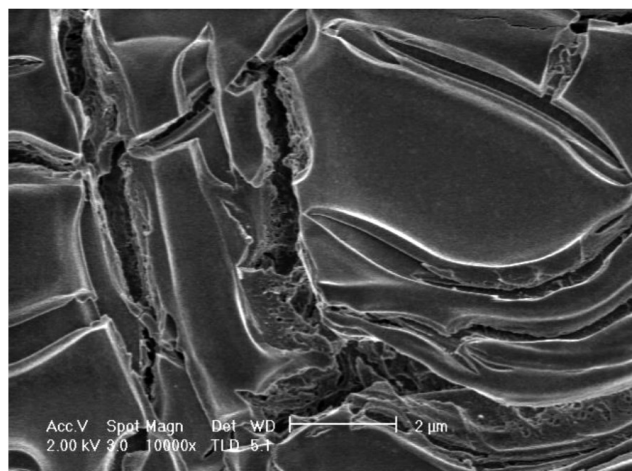


Figure 4: SEM images of the coatings produced with: a) sol-gel and b) PVD

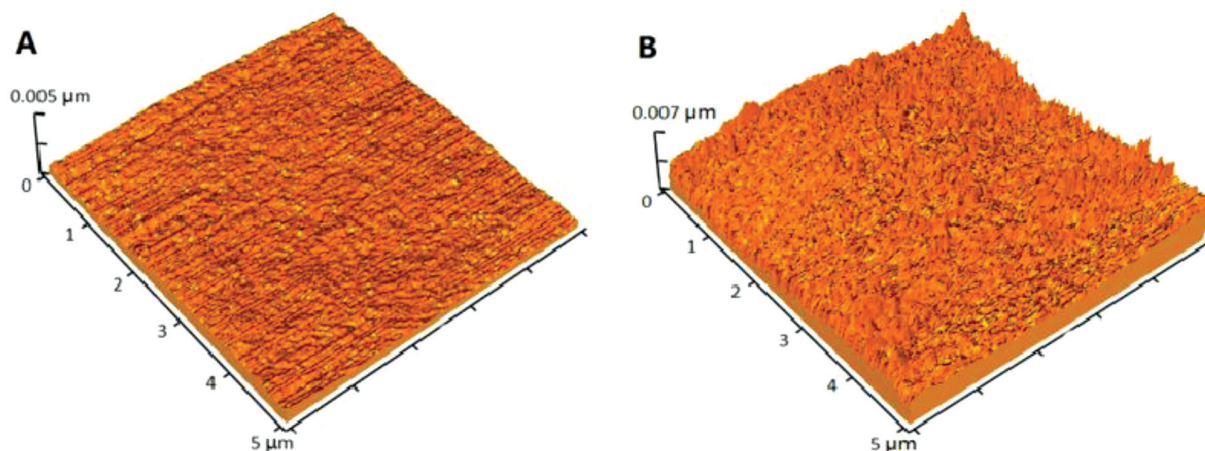


Figure 5: AFM images of the coatings produced by: A) PVD and B) sol-gel

Grain sizes determined with the Sherer method are given in **Table 3**.

Table 3: Average grain sizes of the coatings

Sample	Composition	PVD (nm)	Sol-gel (nm)
1	TiN	14.27	31.02
2	50 % N ₂ – 50 % O ₂	13.64	28.31
3	25 % N ₂ – 75 % O ₂	13.59	24.21
4	15 % N ₂ – 85 % O ₂	13.23	23.30
5	10 % N ₂ – 90 % O ₂	12.21	22.91
6	5 % N ₂ – 95 % O ₂	12.05	18.13
7	Pure TiO ₂	11.79	11,30

Band gap values that occur when the coatings were passed directly and indirectly are shown in **Table 4**.

Table 4: Coatings' band gap values

Sample	Composition	Direct PVD (eV)	Direct-sol-gel (eV)
1	TiN	2.73	3.29
2	50 % N ₂ – 50 % O ₂	2.71	3.21
3	25 % N ₂ – 75 % O ₂	2.96	3.30
4	15 % N ₂ – 85 % O ₂	2.99	3.34
5	10 % N ₂ – 90 % O ₂	2.92	3.33
6	5 % N ₂ – 95 % O ₂	2.85	3.32
7	Pure TiO ₂	0	0

In **Table 5**, degradation rates of the samples exposed to sunlight for 3 h in rhodamine-B, depending on the Ti/N ratios are given.

Table 5: Coatings' band gap values

Sample	Composition	Decomposition (PVD)	Decomposition (sol-gel)
1	TiN	0.68	0.11
2	50 % N ₂ – 50 % O ₂	0.52	0.09
3	25 % N ₂ – 75 % O ₂	0.32	0.07
4	15 % N ₂ – 85 % O ₂	0.23	0.05
5	10 % N ₂ – 90 % O ₂	0.19	0.02
6	5 % N ₂ – 95 % O ₂	0.12	0.01
7	Pure TiO ₂	0	0

Table 6 shows the photoactivity experiment results obtained with PVD and sol-gel.

Table 6: Photoactive dissociation rates of PVD and sol-gel coatings

Sample	Composition	Dissociation percentage (PVD)	Dissociation percentage (sol-gel)
1	TiN	68.1	11.2
2	50 % N ₂ – 50 % O ₂	51.8	8.98
3	25 % N ₂ – 75 % O ₂	32.4	7.01
4	15 % N ₂ – 85 % O ₂	23.1	4.99
5	10 % N ₂ – 90 % O ₂	18.9	1.97
6	5 % N ₂ – 95 % O ₂	11.9	1.11
7	Pure TiO ₂	0	0

AFM images obtained to compare the homogeneities of coatings produced by sol-gel and PVD are shown in **Figure 5**.

4 DISCUSSION

According to the results of the thermogravimetric analysis, there was weight loss due to the evaporation of the remaining water from the solution up to 300 °C; decomposition and combustion of organic components were also observed. A strong exothermic reaction at a peak temperature of 400 °C shows the crystallization of the anatase phase from the amorphous structure. A very low weight loss after 500 °C reveals that the structure consists entirely of TiO₂. It was determined that the low intensity endothermic peak at the 800 °C range belongs to the anatase rutile phase transformation reaction.

As a result of the XRD analysis of the samples heat treated at (400, 500 and 600) °C, it was determined that all the peaks observed belong to the anatase phase of TiO₂ (ICDD: 01-089-4921) and the peak intensities increased with increasing heat treatment temperature. In addition, it was determined that the anatase rutile phase transformation did not occur under the applied heat treatment conditions.

According to the XRD results, it was determined that only the anatase phase crystallized in all undoped and doped samples, and the nitrogen addition did not cause any phase transformation or the formation of a new phase with the selected doping ratios. In addition, it was determined that the nitrogen addition reduced the peak intensities of the anatase phase. The decrease in peak intensities as a result of doping indicates that the degree of crystallinity decreases due to lattice distortion or stress, as stated in the literature²⁴.

According to the particle size results found with the Scherrer method, the particle size of the undoped TiO₂ photocatalysts was approximately 13.5 nm. In the literature, it is mentioned that the anatase phase is more dominant than the rutile phase in structures with particle sizes below 14 nm.²⁵ The facts that only the anatase phase is seen in the structure and that the average particle size values are below this limit confirm this situation. Nitrogen addition was found to increase the particle size. These particle sizes are consistent with the results from the literature.²⁶ The obvious difference between the PVD and sol-gel methods becomes clear after this stage. While the particle size and coating thickness can be kept under control with the PVD method, these values show variability and unusual differences compared with the sol-gel method.

UV-Vis spectra obtained by examining the absorption behaviour of doped and undoped TiO₂ photocatalysts were evaluated and according to the obtained absorption spectra, it was determined that N doping shifts the absorption limit of TiO₂ to higher wavelengths, but significantly reduces the absorption amount of TiO₂ photocatalysts in a wavelength range of 300–500 nm.

When the calculated optical band gap energies of the samples were evaluated, it was determined that N additions increased the band gap energy, and the highest eV values were observed in samples with a 50-% N addition. When the calculated eV values of the thin film samples were compared, it was observed that the band gap energies of the powder samples were lower than those of the thin film samples. In addition, it was determined that the lowest band gap energy values for both PVD and sol-gel samples were obtained for undoped samples, and N-doping increased the band gap energy. When these results were compared with the literature, it was determined that the band gap energy of TiO₂ aligned with the literature values and that non-metallic additives increased the band gap energy to a degree similar to the one observed in this study.²⁷

The photocatalytic activities of thin-film and powdered photocatalysts, used under ultraviolet (UV) and visible light sources, cause the degradation of methylene blue and rhodamine-B. Rhodamine-B photocatalytic degradation is a first-order reaction; its reaction rate (k) is determined according to Equation (6) where C is the rhodamine-B concentration, C_0 is the initial concentra-

tion of rhodamine-B, k is the rate constant, and t is the time.²⁸

$$\ln \frac{C_0}{C} = k \cdot t \quad (6)$$

According to the results obtained, it was determined that the undoped TiO₂ photocatalyst had the highest rate constant under UV light, while the rhodamine-B solution without a photocatalyst had the lowest rate constant. It was determined that the photocatalytic rate constant decreased with the nitrogen addition and the 50 %N-TiO₂ sample had the lowest rate constant.

When the photocatalytic activity results were found for thin films, it was determined that the photocatalytic activity of the TiO₂ thin film coatings made with PVD was quite high compared to the thin film coatings made with sol-gel. When the photocatalytic activity results were determined in general, it was observed that increasing N-ratio increased the photocatalytic activity. The high photocatalytic activity values of thin films, attributed to their large surface area, also align with the calculated optical band gap energy values and results from the literature.²⁹

5 CONCLUSIONS

TiN, Ti-O-N and TiO₂ thin films were applied onto a quartz glass substrate using the cathodic arc PVD and sol-gel methods. All coatings made with the sol-gel method, except for TiN, exhibited an amorphous structure and the anatase phase, which was formed after heat treatment; on the contrary, all coatings made with PVD were detected in the anatase structure.

After the microstructure analysis, it was determined that the surfaces of the coatings produced with sol-gel were heterogeneous, and the grains in their microstructures were larger. The control of the coating thickness was more difficult, and the process took a long time. With both methods, the effect of nitrogen on the photocatalytic activity was clearly observed, and a direct effect of the grain size on the coating quality was identified.

In conclusion, it was proven that this coating can be photoactive under visible light due to nitrogen doping in TiO₂, regardless of the method used. It is clear that the photocatalyst TiO₂, when activated by visible light, will have more applications in daily life. In our world, which has experienced a pandemic such as Covid-19, it finds wide application in areas requiring high levels of hygiene.

Acknowledgement

I would like to thank the ITU Materials Science Laboratory for its support to our project titled “Investigation of Photocatalytic Activity of Nitrogen Doped TiO₂ Coatings Synthesized by Sol-Gel and PVD Methods”, which

was supported within the scope of the R&D Innovation Support Program.

6 REFERENCES

- ¹ B. Akman, B. İslam, G. K. Can, N. T. Avşar, D. Ş. Karaman, E. Baysoy, Gıda ve Sağlık Uygulamaları İçin UV-A Işıma Altında Alternatif Bir Fotokatalizör Olarak: Doğal Melanin Nano-parçacıkları, *Avrupa Bilim ve Teknoloji Dergisi*, 32 (2021), 940–946, doi:10.31590/ejosat.1040830
- ² Y. Ö. Altıntaş, I. Gökçe, M. C. Yıldırım, H. E. Ünalın, S. Sönmezöğlü, T. Öztürk, Yeni nesil Zn₂SnO₄-GO-M (M: Mn, Co) foto katalizör kompozit yapıların sentezi, karakterizasyonu ve antibakteriyel özelliklerinin incelenmesi, *GCRIS*, (2019), 101–123
- ³ M. Bulut, Ü. Birben, AB Su Çerçeve Direktifinin Türkiye’de su kaynakları yönetimine etkisi, *Turkish Journal of Forestry*, 20 (2019) 3, 221–233, doi:10.18182/tjf.562550
- ⁴ F. Dalkılıç, Gözenekli cam üzerine immobilize edilmiş nadir toprak iyonu katkılı TiO₂ ile suların boyar madde giderimi, MS thesis, Konya Teknik Üniversitesi, 2022, 17–35
- ⁵ Y. S. Dewi, Sintesis dan karakterisasi fotokatalis TiO₂ mesopori terdoping galium (III) dengan variasi konsentrasi dopan Ga³⁺ menggunakan metode sonikasi, Diss, Universitas Islam Negeri Maulana Malik Ibrahim, 2019, 103–120
- ⁶ V. Dutta, S. Sharma, P. Raizada, V. K. Thakur, A. A. P. Khan, V. Saini, P. Singh, An overview on WO₃ based photocatalyst for environmental remediation, *Journal of Environmental Chemical Engineering*, 9 (2021) 1, 105018, doi:10.1016/j.jece.2020.105018
- ⁷ Q. Guo, C. Zhou, Z. Ma, X. Yang, Fundamentals of TiO₂ photocatalysis: concepts, mechanisms, and challenges, *Advanced Materials*, 31 (2019) 50, 1901997, doi:10.1002/adma.201901997
- ⁸ G. E. Keleş, Kobalt Ferrit Nano-parçacıkların Sentezi, Karakterizasyonu ve Fotokataliz Uygulamaları: Farklı Çöktürücü Maddelerin ve Yöntemlerin Etkisi, *Journal of the Institute of Science and Technology*, 13 (2023) 1, 432–447
- ⁹ Z. Huang, J. Wang, S. Lu, H. Xue, Q. Chen, M. Q. Yang, Q. Qian, Insight into the real efficacy of graphene for enhancing photocatalytic efficiency: a case study on CVD graphene-TiO₂ composites, *ACS Applied Energy Materials*, 4 (2021) 9, 8755–8764, doi:10.1021/acsaem.1c00731
- ¹⁰ M. S. İzgi, C. Zörer, O. Baytar, Ö. Şahin, S. Horoz, Etkili Aktif Karbon Destekli CdS Fotokatalizörlerin Fotokatalitik Uygulamaları, *Bitlis Eren Üniversitesi Fen Bilimleri Dergisi*, 9 (2020) 2, 662–670, doi:10.17798/bitlisfen.642608
- ¹¹ X. Liu, M. Sayed, C. Bie, B. Cheng, B. Hu, J. Yu, L. Zhang, Hollow CdS-based photocatalysts, *Journal of Materiomics*, 7 (2021) 3, 419–439, doi:10.1016/j.jmat.2020.10.010
- ¹² C. M. Magdalane, G. M. A. Priyadharsini, K. Kaviyarasu, A. I. Jothi, G. G. Simiyon, Synthesis and characterization of TiO₂ doped cobalt ferrite nanoparticles via microwave method: Investigation of photocatalytic performance of congo red degradation dye, *Surfaces and Interfaces*, 25 (2021), 101296, doi:10.1016/j.surfin.2021.101296
- ¹³ M. K. A. Mohammed, Sol-gel synthesis of Au-doped TiO₂ supported SWCNT nanohybrid with visible-light-driven photocatalytic for high degradation performance toward methylene blue dye, *Optik*, 223 (2020), 165607
- ¹⁴ N. Özdoğan, K. Özdemir, İçme suyu kaynaklarındaki trihalometan oluşumunun incelenmesi, *Avrupa Bilim ve Teknoloji Dergisi*, 17 (2019), 776–785, doi:10.31590/ejosat.635926
- ¹⁵ C. Özgür, Dezenfeksiyon ünitesi risk analizi: içme suyu arıtma tesisi, *Niğde Ömer Halisdemir Üniversitesi Mühendislik Bilimleri Dergisi*, 10 (2021) 1, 16–22
- ¹⁶ S. P. Luberty Sinaga, S.i P. Rasio Dopan. Fe₂O₃ dan Temperatur Kalsinasi Terhadap Karakteristik Komposit TiO₂/Fe₂O₃ sebagai Material Fotokatalis, Diss., Universitas Brawijaya 2021
- ¹⁷ B. Pant, M. Park, S. Park, Recent advances in TiO₂ films prepared by sol-gel methods for photocatalytic degradation of organic pollutants and antibacterial activities, *Coatings*, 9 (2019) 10, 613
- ¹⁸ S. Patial, V. Hasija, P. Raizada, P. Singh, A. A. P. K Singh, A. M. Asiri, Tunable photocatalytic activity of SrTiO₃ for water splitting: strategies and future scenario, *Journal of Environmental Chemical Engineering*, 8 (2020) 3, 103791, doi:10.1016/j.jece.2020.103791
- ¹⁹ A. Vahl, S. Veziroglu, B. Henkel, T. Strunskus, O. Polonskyi, O. C. Aktas, F. Faupel, Pathways to tailor photocatalytic performance of TiO₂ thin films deposited by reactive magnetron sputtering, *Materials*, 12 (2019) 17, 2840, doi:10.3390/ma12172840
- ²⁰ Y. Wang, K. H. Rahman, C. C. Wu, K. C. Chen, A review on the pathways of the improved structural characteristics and photocatalytic performance of titanium dioxide (TiO₂) thin films fabricated by the magnetron-sputtering technique, *Catalysts*, 10 (2020) 6, 598, doi:10.3390/catal10060598
- ²¹ A. Ali Yaqoob, N. H. B. Mohd Noor, A. Serra, M. N. Mohamad Ibrahim, Advances and challenges in developing efficient graphene oxide-based ZnO photocatalysts for dye photo-oxidation, *Nanomaterials*, 10 (2020) 5, 932, doi:10.3390/nano10050932
- ²² X. Zhang, G. Lu, X. Ning, C. Wang, Boron substitution enhanced activity of B_xGa_{1-x}As/GaAs photocatalyst for water splitting, *Applied Catalysis B: Environmental*, 300 (2022), 120690, doi:10.1016/j.apcatb.2021.120690
- ²³ V. Gombac, L. DeRogatis, A. Gasparotto, G. Vicario, T. Montinia, D. Barreca, G. Balducci, P. Fornasiero, E. Tondello, M. Graziani, TiO₂ nanopowders doped with boron and nitrogen for photocatalytic applications, *Chemical Physics*, 339 (2007), 111–113
- ²⁴ D. A. H. Hanaor, C. C. Sorrell, Review of the anatase to rutile phase transformation, *Journal of Materials Science*, 46 (2011), 855–874, doi:10.1016/j.chemphys.2007.05.024
- ²⁵ H. Z. Zhang, J. F. Banfield, Thermodynamic analysis of phase stability of nanocrystalline titania, *Journal of Materials Chemistry*, 8 (1998), 2073–2076, doi:10.1039/A802619J
- ²⁶ V. Gombac, L. DeRogatis, A. Gasparotto, G. Vicario, T. Montinia, D. Barreca, G. Balducci, P. Fornasiero, E. Tondello, M. Graziani, TiO₂ nanopowders doped with boron and nitrogen for photocatalytic applications, *Chemical Physics*, 339 (2007), 111–113, doi:10.1016/j.chemphys.2007.05.024
- ²⁷ A. Zaleska, J. W. Sobczak, E. Grabowska, J. Hupka, Preparation and photocatalytic activity of boron-modified TiO₂ under UV and visible light, *Applied Catalysis B: Environmental*, 78 (2008), 92–100, doi:10.1016/j.apcatb.2007.09.005
- ²⁸ A. Houas, H. Lachheb, M. Ksibi, E. Elaloui, C. Guillard, J. M. Herrmann, Photocatalytic Degradation Pathway of Methylene Blue in Water, *Applied Catalysis B: Environmental*, 31 (2001), 145–157, doi:10.1016/S0926-3373(00)00276-9
- ²⁹ J. H. Xu, J. Li, W. L. Dai, Y. Cao, H. Li, K. Fan, Simple fabrication of twist-like helix N, S-codoped titania photocatalyst with visible-light response, *Applied Catalysis B: Environmental*, 79 (2008), 72–80, doi:10.1016/j.apcatb.2007.10.008